CLM - R 152

CULHAM LIBRARY
REFERENCE ONLY

CULHAM LABORATORY
LIBRARY
- 4 MAY 1976
b
L

CLM - R 152

UKAEA RESEARCH GROUP

Report

REVIEW OF IRRADIATION CREEP AND SWELLING IN A FUSION REACTOR BLANKET CELL STRUCTURE

J R STANBRIDGE
H A SHOTTER

CULHAM LABORATORY
Abingdon Oxfordshire
1976

Available from H. M. Stationery Office

C/18

£1.00

Enquiries about copyright and reproduction should be addressed to the Librarian, UKAEA, Culham Laboratory, Abingdon, Oxon. OX14 3DB, England.

UDC
621.039.634:669-179

REVIEW OF IRRADIATION CREEP AND SWELLING IN A FUSION REACTOR BLANKET CELL STRUCTURE *

by

J.R. Stanbridge

H.A. Shotter

Associated Nuclear Services, Epsom, UK

ABSTRACT

This report is a continuation of previous work aimed at determining the limiting performance of a fusion reactor blanket cell as a function of its life.

The fusion reactor is assumed to be lithium-cooled with cylindrical geometry blanket cells having stainless steel walls. Their performance is limited by irradiation creep strain which occurs as a result of the internal coolant pressure. The report reviews some of the competing mechanisms for irradiation creep strain and makes estimates of creep using the hypothesis of Brailsford and Bullough in which irradiation creep is a function of temperature rather similar to the temperature variation of swelling. Estimates are made of the irradiation damage-rates both axially and circumferentially for the cell. For a 5 year cell life the introduction of the temperature variation of irradiation creep causes the previous estimate of wall loading to be reduced by nearly 20%, to 1.8 MW/m^2.

* The work was carried out by Associated Nuclear Services under Culham Contract No. MIA 67398.

UKAEA Research Group,
Culham Laboratory,
Abingdon,
Oxon.
(Euratom/UKAEA Fusion Association)
September 1975

SBN 85311 040 9

CONTENTS

NOTATION

b	Bergers Vector		T	temperature K
d	void diameter (cell diameter in Appendix D)		D(T), E(T), K(T)	function of temperature in the expression for swelling
D	no. of atomic displacements dpa/MW/m^2/yr		V	volume
f	a stress function in the expression for irradiation creep (solid fraction of neutron path in Appendix B)		W	reactor thermal wall loading MW/m^2
			ϵ	creep strain %
K	Boltzman's constant		ρ	void number density
l	radial distance into blanket from front wall		ϕt	fluence n/cm^2
n	number of atoms in an interstitial loop nucleus		α	angle to normal at which a neutron strikes inner wall
p	cell internal pressure		σ	stress MN/m^2
r_p	minor radius of plasma m		τ	time yrs
r	minor radius of torus to inner wall (radius of element in Appendix B) m		ϕ_{pl}	14MeV flux at depth l from front wall
			ϕ_{sl}	non 14MeV flux at depth l from front wall
R	major radius of torus m			
t	cell wall thickness cm		S	first wall 14MeV current density

1. INTRODUCTION

The work reported here primarily comprises a review of irradiation creep and swelling data which could be applied to the design of fusion reactor blanket cells. It is a sequel to a previous investigation (Ref. 1) which concluded that the maximum blanket cell wall loading was a function of its life and was limited by irradiation creep strain. An empirical relationship was used for irradiation creep strain which was independent of temperature.

A brief review is given here of competing irradiation creep hypotheses which are still controversial and a particular theory, by Brailsford and Bullough, for which there is some experimental support, is used to make revised cell life estimates. They postualte that irradiation creep is due to the preferred orientation of irradiation-produced interstitial loops. The creep is proportional to the swelling rate, which is a function of temperature.

In another section of the report the variation of neutron flux, and hence damage rate round the circumference at different points along the axis of cylindrical blanket cells, is examined.

2. LITERATURE SURVEY OF IRRADIATION CREEP AND SWELLING MODELS

2.1 Irradiation creep

This and subsequent sections of the report are in the nature of a review of the irradiation creep and swelling calculations reported in ref. 1, in an attempt to improve on that work which was based on an empirical relationship for irradiation creep from data obtained at about 250°C. The review will attempt to determine whether irradiation creep is temperature dependent, and if so, how it should be extrapolated with temperature.

The review begins with a brief summary of the possible irradiation creep mechanisms which are surveyed in a paper by Gilbert (Ref. 2) and a later one by Hesketh (Ref. 3). First it is worth echoing the chairman's closing remarks to the BNES Conference on Irradiation Embrittlement and Creep (1972), indicating the dearth of data at higher doses and higher temperatures and also pointing out the problem of determining the ductility of a material which is deformed by a combination of thermal and irradiation creep. If published information is anything to go by these remarks are still true today, and they are of course particularly relevant to the application on the fusion reactor.

Irradiation creep in this report is taken to mean a time dependent deformation of a material under an applied stress, resulting from irradiation. An essential feature is that the stress sensitivity of the strain rate is flux dependent. Irradiation creep mechanisms are based on the common feature of Frenkel-pair generation from neutron-atom interactions and the separation of these into clusters through neutron- and fission-produced displacement spikes, and diffusion.

Spike mechanism

This is described as the relaxation of elastic strains by hot spots (neutron or fission fragment spikes). Creep by this mechanism would be linear in stress and insensitive to temperature. Hesketh tends to discount this mechanism in his review on the basis of the experimental evidence.

Yielding creep

This is described in some detail by both Gilbert and Hesketh. It appears to describe satisfactorily irradiation creep in non-cubic materials such as uranium and zirconium. Anisotropic irradiation growth leads to internal stresses building up between grains which eventually lead to plastic yielding. As Hesketh explains this mechanism cannot account for irradiation creep in cubic materials.

Loop orientation

This model, due to Hesketh, is the collapse of clusters of irradiation-produced defects (vacancy cascades) into dislocation loops aligned preferentially on the available crystallographic planes under the influence of applied stress. Hesketh himself discounts this mechanism because of the large number of vacancies (200) which must neatly collapse.

Loop unfaulting

Dislocation loops in close-packed structures are generally faulted and cannot glide. At high temperatures these dislocations grow by absorbing point defects until they reach a critical radius when it is energetically favourable for them to glide. Hesketh reports that loop unfaulting is unlikely to begin until after a threshold dose of 10 dpa and then only at temperatures in excess of 500°C. From results quoted later in this work it may be concluded that the front wall may reach this dose after about one year's operation, but it is only at the back end of a cell that the temperature will approach 500°C and at this point the damage rate is reduced by about a factor 10. This mechanism would therefore not contribute significantly to irradiation creep in a fusion reactor, with stainless steel as the blanket structural material. Its significance with other materials would also depend on the threshold dose and temperature.

Dislocation climb

The models which have been proposed suggest an enhancement of the thermal creep rate by irradiation enhancement of vacancy diffusion. These models have been criticised by Mosedale and Hesketh on the grounds that diffusion of defects produced by irradiation is independent of stress.

Preferred nucleation and growth of interstitial loops

In their paper, Brailsford and Bullough (Ref. 4) concentrate on two mechanisms - the preferential nucleation of irradiation-produced interstitial loops oriented perpendicular to the tensile

stress axis, and the subsequent growth of these loops once the nucleation stage is terminated. Their calculation indicates the relative importance of each mechanism. It is concluded that the creep strain resulting from the enhanced growth of favoured loops is negligible compared to that arising from their preferred nucleation, at temperatures below the temperature at which the maximum swelling rate occurs. Up to this temperature the creep rate is simply related to the volume swelling rate

$$\frac{d\varepsilon}{dt} = f \times \left(\frac{\text{total dislocation density}}{\text{total dislocation density in the form of interstitial loops}} \right) \times \frac{d}{dt} \left(\frac{\Delta V}{V} \right) \quad (1)$$

where

$$f = \frac{\exp\left[.\sigma b^3 n/KT\right] - 1}{\exp\left[\sigma b^3 n/KT\right] + 2}$$

It is assumed in the calculations that the second term in the above equation is approximately equal to unity, i.e. that all the dislocations occur in interstitial loops. Because irradiation creep results only from irradiation-produced dislocation loops the term

$$\frac{d}{dt} \left(\frac{\Delta V}{V} \right)$$

is the void swelling rate and not the total swelling rate including helium production.

With these assumptions, equation (1) will be used to calculate irradiation creep strains in the blanket cell. The summaries of some of the competing irradiation creep mechanisms are included above in order to sound a cautionary note that the subject is still highly controversial. It is also worth noting here some of the discussion which has appeared in the literature concerning this particular mechanism. Some of this has centred round the lack of evidence for any temperature dependence of irradiation creep.

Mosedale et al (Ref. 5) attempt to explain their results in terms of this theory but find it necessary to put $n \sim 80$ for agreement, which they find unrealistic. They therefore attribute most of the strain to some other, unidentified mechanism. In a similar exercise, Lewthwaite (Ref. 6) concludes that it is necessary either to abandon the concept of equality of numbers between vacancies in voids and interstitials in loops, i.e. the relationship between creep and swelling, or to assume that an interstitial loop nucleus contains about 30 atoms.

Work by Okamoto and Harkness (Ref. 7) to measure the Frank loop size distribution and concentration on each set of (111) planes showed that the average loop size is the same on these planes but the loop concentration varied by a factor approximately 2. This result tends to support the mechanism of Brailsford and Bullough. Herschbach and Schneider (Ref. 8) have reassessed the connection between irradiation creep and swelling making different statistical assumptions and they conclude that their results also tend to support the theory.

2.2 Swelling

The effects of fast neutron irradiation on void formation in solution treated Type 316 stainless steel up to a peak fluence of 5.1×10^{22} n/cm^2 and at temperatures between 0.39 and 0.67 Tm have been investigated by Brager and Straalsund (Ref. 9). The irradiations were carried out in three irradiation pins in equivalent Row II positions in the EBR-II reactor. In the previous work (Ref. 1) an empirical equation by Claudson for 20% cold worked Type 316 stainless steel was used. Now the present investigation has not included an investigation of the relative merits of cold worked or annealed material but is aimed at exploring other variables such as temperature. Claudson did not explicity state in his report the range of temperature and fluence of the data on cold worked material, although his data points for annealed material covered a similar range to those above for Brager and Straalsund. It was however agreed that for the present investigation the Brager and Straalsund equation would be used. The empirical relationship for void swelling developed by them is as follows:-

$$\Delta V/V = \tfrac{1}{6}\pi \times 10^{-9} K(T) \rho d^3$$

$$= \tfrac{1}{6}\pi \times 10^{-9} K(T) \left[(\phi t)^{D(T)} \exp\left\{ E(T) \right\} \right] \quad (2)$$

where

$\Delta V/V$ = void volume (%),

$K(T)$ = ratio of the mean of the void diameter cubed $(\bar{d}^3)$ to the cube of the mean void diameter $(\bar{d})^3$,

$= 0.48 + 9.2 \times 10^{-4} T$ for $T < 873$,

$= 1.28$ for $T > 873$,

$D(T) = 0.72 + \left[1.7 / \left\{ 1 + \exp(0.04\ [700 - T]\ ) \right\} \right]$,

$E(T) = 49.46 - 0.02432T - 944/T$

This expression will be used to evaluate the term $\Delta V/V$ in the calculation of irradiation creep. The expression was derived from data in an environment where helium bubble formation was insignificant and it may not therefore accurately predict swelling in a fusion reactor structure. This problem is discussed by Wiffen and Bloom (Ref. 10) who refer to a model by Barnes (Ref. 11) which assumed that the swelling depends on the helium content and in which the cavities are equilibrium bubbles. The difficulty in applying Barnes model for swelling is in determining with confidence the values of some of the parameters which must be fed into the equation.

Wiffen and Bloom assume a cavity concentration independent of irradiation temperature of 10^{14}cm^{-3} and Barnes himself suggests a surface energy 1000 ergs/cm^2. The other difficult parameter is the surface self-diffusion coefficient for which we have not been able to find reliable values. In view of the uncertainties it is doubtful whether predictions using this model have any practical value.

3. EXTENT OF NEUTRON FLUX AND DAMAGE VARIATIONS WITHIN A BLANKET CELL WALL

3.1 General object

The purpose of this section is to examine the possible extent of the axial and circumferential variation in damage rate which can occur in the side wall of a cylindrical cell used as a basic constructional element of the blanket in the manner indicated by Fig. 1.

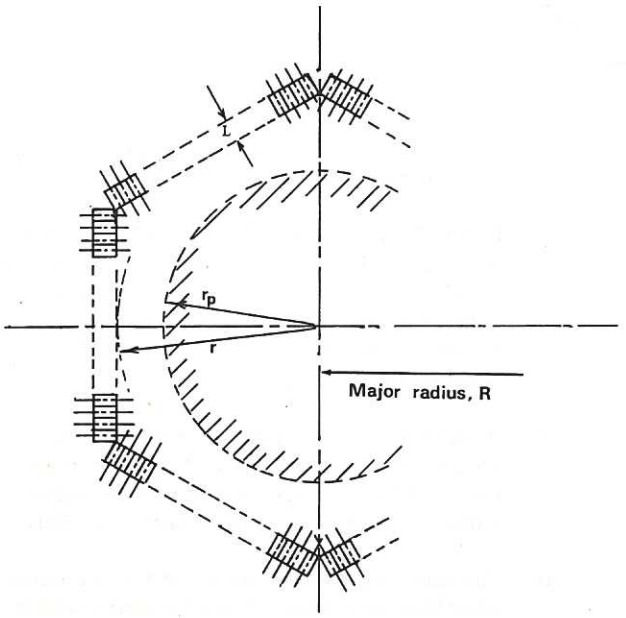

Fig.1 Proposed form of construction of cellular blanket.

3.2 Basic data and assumptions

As shown in Fig. 1 the form of blanket construction envisaged employs close-packed cylindrical cells, 0.3 m diameter, which are assembled so that the surface exposed to the plasma, (the 'front wall'), forms an enclosure which is hexagonal in form when viewed in a direction lying along the plasma axis. Thus, except at the hexagon vertices, the intercellular spaces are of constant shape and cross-section throughout their length. (Non-cylindrical cells, shaped to minimise neutron leakage, are assumed to exist at the hexagon vertices, but are not here examined.)

The general level of voidage existing within the blanket structure is taken to be that produced by perfectly packed cylinders, viz, 9.3% of total volume (see fig. 2).

Basic system dimensions, (whose definitions are indicated in Fig. 1), are as follows:

Torus major radius, R,	= 16.73m
Plasma minor radius, r_p,	= 4.15m
(Equivalent torus minor radius, (inner wall)), r	= 5.8 m
Blanket radial depth, L,	= 0.6 m

As is apparent in Fig. 1, cell-groups situated near to the mid-point of each side of the hexagon will experience a considerably greater degree of streaming of 14 MeV neutrons from the plasma through the intercellular passages than do those situated near to the hexagon vertices. In consequence it is these cells which will experience the greatest amount of side-wall damage rate due to this streaming and also the greatest circumferential variation in side-wall damage rate at any given axial depth. This variation follows from the fact that a greater proportion of the flight-paths of the streaming neutrons will terminate near to the most exposed point of the cell-wall circumference than will terminate near to the contact point with the neighbouring cell.

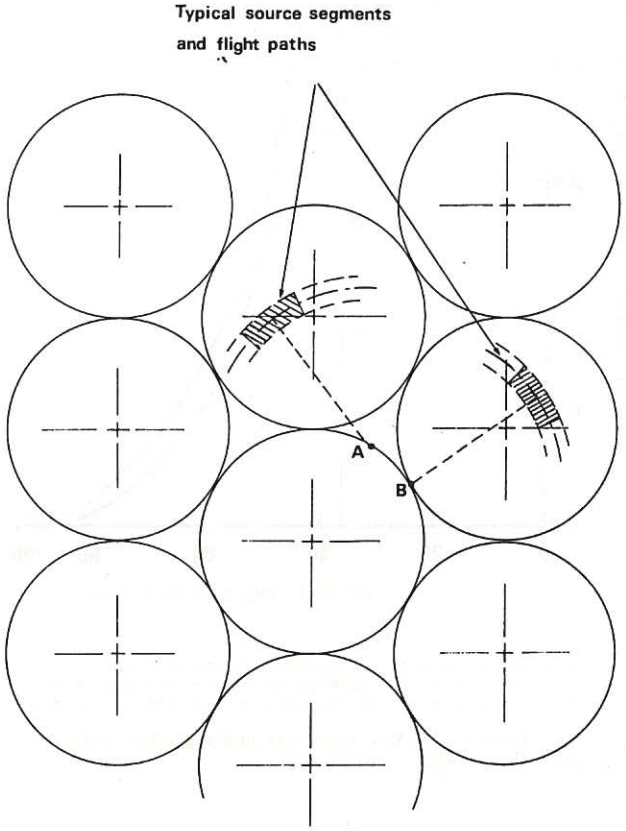

Fig.2 Elevation of blanket used for determining voided fraction of neutron flight paths.

Attention in this report is therefore restricted to analysing conditions in these more centrally located cells.

Finally, for the purposes of a streaming calculation it is necessary to specify the angular distribution of 14 MeV plasma neutrons arriving at any particular point in the first wall. This distribution has a complex form which, because of the toroidal geometry, varies with the position of incidence around the hexagonal periphery and at any position is azimuthally non-uniform with respect to the wall normal. The precise shapes of these distributions at the innermost and outermost points on the first wall minor circumference have been calculated by Dänner (Ref. 12) for a system which assumes a uniform neutron source within the plasma and which has geometric proportions differing only slightly from those here employed, (r_p/r = 0.8 rather than 0.716). Figure 3 shows plots of these two 14 MeV neutron current distributions as a function of angle of incidence, obtained by azimuthally averaging the Dänner data at

the two points concerned, and converting resultant fluxes into wall-current density values using the relation $j = \phi \cos\alpha$. Figure 3 also shows a plot of the azimuthally invariant 14 MeV current distribution actually assumed in the calculation now reported.

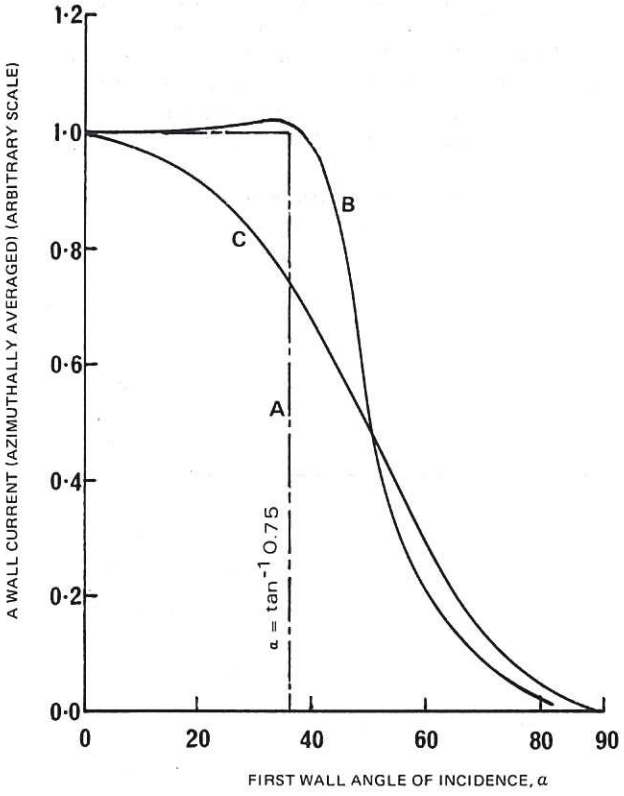

CURVE 'A' : Report 'reference' distribution
" 'B' : Ref. 12 distribution for outermost cell
" 'C' : Ref. 12 distribution for innermost cell

Fig.3 Variation of 14 MeV current with angle of incidence at given points on front wall.

It can be seen from Fig. 3 that in comparison with the two calculated distributions this assumed distribution is more centrally concentrated, and therefore suitable as a basis for pessimistic estimation of neutron streaming effects from a uniform plasma source.

3.3 Calculational procedure

Owing to the complex nature of the neutron source geometry and of the blanket slowing-down process, a full analysis of the variation through the blanket of the neutron flux and its associated spectrum was not regarded as within the scope of the present work. Instead, a starting point was taken to be the results of corresponding calculations for a homogeneous, (i.e. non-cellular), blanket derived by the Monte Carlo code SPECIFIC and made available by G. Constantine, AERE. These comprised flux values for the 14 MeV energy group and for 36 "slowing-down" groups at the front, side, and rear walls of an unvoided blanket of thickness and neutron source shape similar to that under consideration, (originally supplied as supporting data for Ref. 1). Although calculated for a niobium-walled blanket these results are considered to represent those obtaining in the stainless steel system sufficiently for present purposes.

These data, when normalised to a front wall loading of 1 MW/m^2, (defined on a basis of 20.2 MeV/fusion event), are shown in Table 1.

Table 1. Unvoided blanket, flux data

Depth into blanket, mm:	0	250	600
14 MeV flux, n/cm^2 sec:	0.52×10^{14}	0.092×10^{14}	0.012×10^{14}
Total flux 14 - 0.1 MeV, n/cm^2 sec:	1.73×10^{14}	0.85×10^{14}	0.29×10^{14}

The derivation of the circumferential variation of irradiation damage rate around a cell wall followed the calculational route set out below.

(i) The 14 MeV flux at various depths of interest through the blanket was found for the assumed angular distribution of incident neutrons defined above (Fig. 3), and using an effective scattering mean free path, l_c = 17.5 cm determined in Ref. 1.

(ii) A 14 MeV neutron damage-rate for these positions was then obtained by multiplying these 14 MeV fluxes by the corresponding IAEA recommended cross-sections (Ref. 13).

(iii) The non-14 MeV damage-rate for the same positions was found by a procedure making use of neutron diffusion theory to effect a suitable interpolation of non-14 MeV flux between the points quoted in Table 1, at which its values were supplied. The 14 MeV flux shape found in (i) above was used as source term in this calculation which is more fully described in Appendix B.

Results from (i), (ii), and (iii) for the part of the blanket of interest are given below:-

Table 2. Unvoided blanket, calculated damage data

Depth into blanket, mm:	0	62.5	125	187.5	250
14 MeV Damage-rate: (Dpa/MWm^{-2}y)	3.47	2.22	1.49	0.94	0.61
Non-14 MeV Damage-rate: (Dpa/MWm^{-2}y)	2.41	2.28	2.06	1.74	1.46

(iv) The final step was to convert the damage data of Table 2 to be applicable to the cellular blanket described above and to make estimates of the maximum and minimum damage-rates in the cell wall, i.e. at points 'A' and 'B' in Fig. 2, at various depths into the blanket.

This circumferential variation between

maximum and minimum points could reasonably be presumed to be due predominantly to the 14 MeV flux component (on account of its highly directional nature and consequent strong streaming tendency). Assuming the 'reference' angular distribution of neutron flight paths shown in Fig. 3, a graphical procedure described in Appendix A was used to evaluate the maximum (point 'A') 14 MeV fluxes and consequent damage-rates at the depths of interest. It was realised however, that application of the same azimuthally uniform distribution to point 'B' neutron flight paths might cause unduly high values of minimum damage-rate to be predicted because of the obvious sensitivity to azimuthal variation existing at this point. Thus to ensure a maximum estimate of circumferential damage variation being made, the point 'B' damage estimates were in the first place taken to be the minimum possible i.e. those which would be produced at a corresponding depth into an unvoided blanket also having the 'reference' form of incident neutron distribution.

The maintenance of an unchanged rate of blanket heat generation in going from solid to cellular forms of construction within the same bounded volume, requires that the blanket thickness be increased to compensate for the reduced mean density of blanket material. The consequence of the reduced blanket density is a progressive relative increase in the non-14 MeV neutron flux through the blanket (Ref. 14). This effect is of relatively minor significance to the cell wall life estimates described later and it has therefore been simplified to the assumption that the non-14 MeV flux remains unchanged at the first wall but is increased in the ratio of the density reduction at points through the wall.

The maximum-to-minimum variations in circumferential damage-rate due to the 14 MeV component, calculated as described, is presented in Table 3 below, together with the associated non-14 MeV component of damage-rate augmented in the above manner.

Table 3. Cellular blanket - variation of 'maximum' and 'minimum' damage with depth

Depth into blanket, mm:		0	62.5	125	187.5	250
'Maximum' point damage (dpa/MWm^{-2} y)	14 MeV	3.47	2.95	2.22	1.60	1.11
	non-14 MeV	2.41	2.51	2.27	1.92	1.61
	Total	5.88	5.46	4.49	3.52	2.72
'Minimum' point damage (dpa/MWm^{-2} y) (Minimum Estimate - see Section 4.3)	14 MeV	3.47	2.22	1.49	0.94	0.61
	non-14 MeV	2.41	2.51	2.27	1.92	1.61
	Total	5.88	4.73	3.76	2.86	2.22

3.4 Discussion of Section 3 results

The values of cell wall circumferential variation in damage-rate listed in Table 3 are maximum estimates both in respect of the position of the cell examined and of the assumptions made in simplifying the calculations.

It can be seen that the peaking of this circumferential variation as distance along the cell axis is varied, is not very pronounced, and that a reasonable maximum estimate for the value of the peak variation itself would be 0.8 dpa/MWm^{-2} y, occurring at a depth of about 100 mm from the first wall.

Significant downward modification of the Table 3 damage-rate variation values and of their associated peak value would result if more refined calculations were carried out making fewer simplifying assumptions, and at the same time taking precise account of the geometry of each individual cell position considered. The more important effects concerned are listed below in approximate descending order of effect.

(i) Use of an accurate form for the angular distribution of 14 MeV neutrons incident at the first wall, taking specific account of its azimuthal variation about the first wall normal. In particular, this would make unnecessary the assumption of an 'all-solid' path for neutrons arriving at the 'minimum' point of the cell circumference. An approximate estimate of this effect has indicated that this would decrease the estimate of peak circumferential damage-rate variation calculated above by about 30%, (mainly due to increase in estimated 'minimum' point damage rate, rather than to decrease in the 'maximum' point estimate).

(ii) Examination of a cell situated in a non-central position of the hexagon outer side. Although this would result in a reduced estimate of peak circumferential variation in damage-rate, there would be an increase (relative to a centrally situated cell) in the peak value of damage-rate variation in the axial direction, which would require appraisal.

(iii) Examination of a cell situated at the centre of the inner rather than the outer vertical side of the hexagon, in which position a correspondingly wider angular distribution of incident 14 MeV neutrons would apply due to the major curvature of the system. A rough estimate using azimuthally averaged forms of the angular distribution data of Dänner plotted in Fig. 3 indicated that in this position there would be a peak circumferential variation about 14% less than that calculated for a cell at the centre of the outer side.

4. CALCULATION OF IRRADIATION CREEP IN BLANKET CELL STRUCTURE

4.1 Cell operating conditions

The basis of the method is to use equation (1) for irradiation creep, substituting equation (2) for the swelling rate. Equation (2) includes a flux dependence, which is really a displacement damage dependence and it will be rewritten in this form in order to enable the extrapolation in damage to fusion reactor conditions to be made, i.e.

$$(\phi t) = k(D\tau)$$

where k is a constant (neutrons/cm^2 per atomic

displacement) and D the atomic displacements/yr, t and τ are both time but in seconds and years respectively. Now in order to determine the value of k it will be assumed that the damage-rate of 60 dpa/yr quoted for EBRII in Ref. 10 corresponds to the maximum test flux position quoted in Ref. 9 where the neutron flux is $1.78 \times 10^{15} n/cm^2 s (E > 0.1 MeV)$.

$$\text{Then } k = 9.356 \times 10^{-2} n/cm^2/.dpa$$

For a calculated fusion reactor blanket damage-rate of D dpa/MW/m^2 yr and a wall loading of W MW/m^2, for substitution in the swelling equation (2) we have

$$\phi t = k.(WD\tau) \qquad (3)$$

Some further discussion is necessary at this point concerning the damage parameter D. The value calculated in our earlier paper is 4.9 dpa/yr MW/m^2 at the front wall. On the face of it this is very much lower than the values quoted in Ref. 15 of ~ 10 dpa/yr/MW/m^2 for the Wisconsin UWMAK, but this figure is for neutronic wall loading and the Wisconsin figure reduces to about 6.8 dpa/yr/MW/m^2 when converted to thermal wall loading.

Our figure was based on displacement cross-sections which were only quoted up to a value 3.68 MeV, but replacing these with the IAEA recommended values of displacement cross-section, which are not significantly different from the Half-Nelson values but go up to the high energy levels, gives the displacement damage-rates quoted in Table 3 i.e. 5.88 dpa/yr/MW.m^2.yr at the front wall. This is in reasonable agreement with the figure quoted for UWMAK above.

The temperature distribution along the axis of the cell was investigated in Appendix 1 of Ref. 1. The cell structure temperatures using this method are shown as a function of wall loading in Fig. 4. The limiting condition chosen is that the maximum structure temperature does not exceed 500°C. This is indicated (Ref. 1) as a probable limit for corrosion between lithium and a stainless steel structure, and furthermore the validity of the irradiation creep relation (equation (1)) is doubtful at temperatures greater than the temperature at which the peak swelling occurs which is in the region of 500°C.

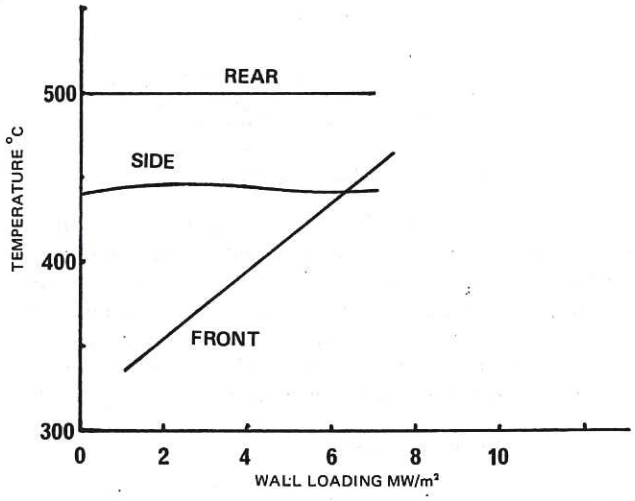

Fig.4 Blanket cell structure mid-wall temperature.

4.2 The application of the Brailsford and Bullough model

Lewthwaite (Ref. 6) attempts to establish a relationship between irradiation creep and swelling, and in fitting this to the experimental data he finds that it is necessary either to abandon the postulate the equality of numbers between vacancies in voids and interstitials in loops, or alternatively, it is necessary to assume that an interstitial loop nucleus contains about 30 atoms. Brailsford and Bullough suggest a figure of 10 for the number of atoms in an interstitial loop nucleus. Now the effect of these two alternative assumptions is shown in Fig. 5, for a wall loading of 2MW/m^2 and a dwell time 5 years. With n = 30 the agreement with the previous results at 300°C is good, but the difference in the strain predictions for the different assumptions is large, particularly at the higher temperatures. In the strain predictions which follow it will be assumed that n = 30 which, if the model is right, is more restrictive on wall loading.

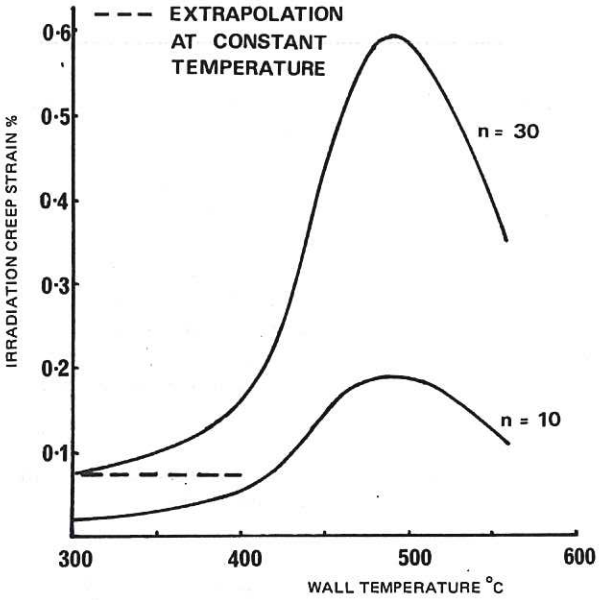

Fig.5 Alternative front wall irradiation creep predictions (wall loading 2 MW/m^2 life 5 years).

4.3 Results

The calculational procedure is described in Appendix C. The calculations assume a cylindrical cell geometry having a diameter 30 cm as described in Ref. 1. The results are presented in the form of constant strain lines for 0.1%, 0.2%, 0.5% and 1% irradiation creep strain which have been calculated for the front, side and rear wall positions, and are shown on Figs. 6, 7, and 8 as a function of cell life and wall loading. The 0.1% strain lines from each of these figures have been replotted on Fig. 9 so that the variation of strain with position can be seen and information is also given to enable a comparison to be made with the previous results presented in Ref. 1. The damage rates used in these calculations are the maximum damage rates for a homogenous blanket. The results of the work described in Section 3 indicate the extent of flux variation around a cell in a design with cylindrical cells which is estimated to have a maximum value at a position about 10 cm in from the front wall. The 0.1% strain lines corresponding to this position are shown in Fig. 10.

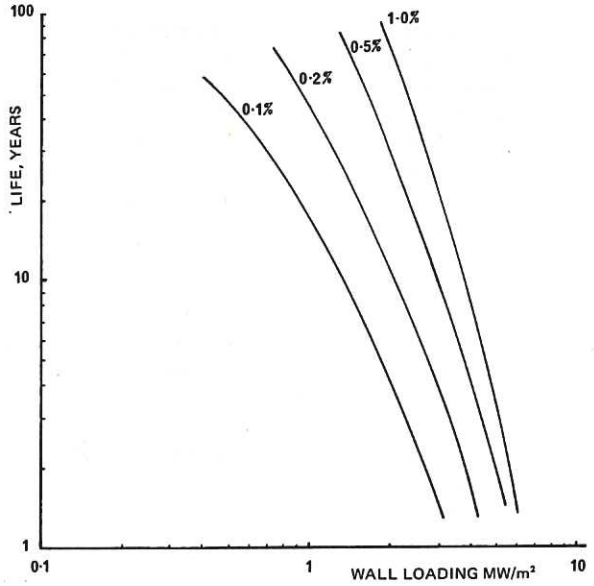

Fig.6 Front wall irradiation creep strain.

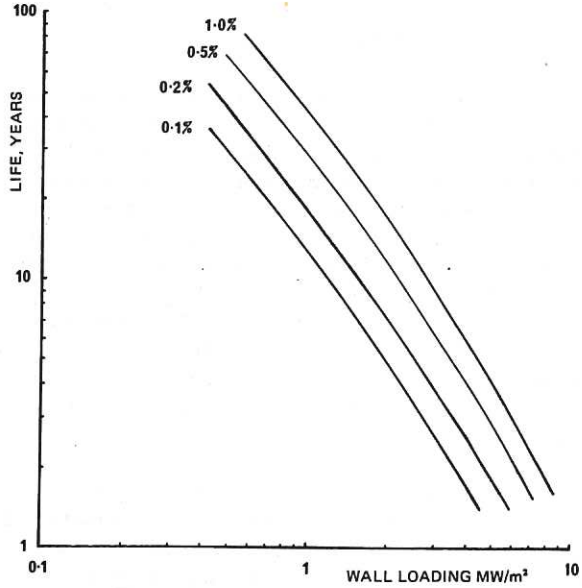

Fig.7 Side wall irradiation creep strain.

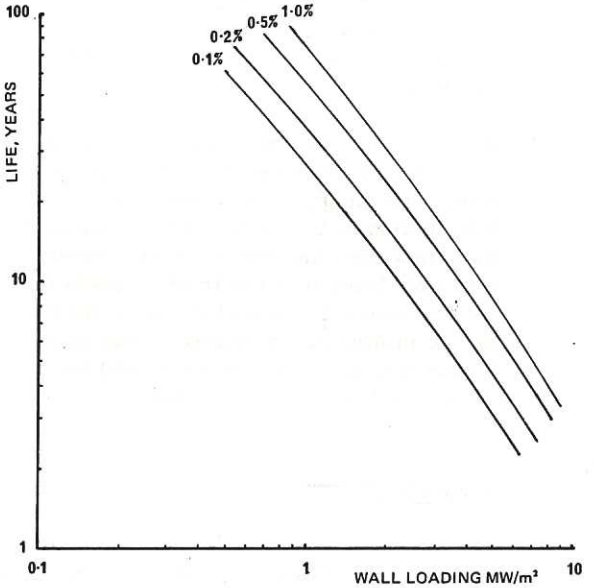

Fig.8 Rear wall irradiation creep strain.

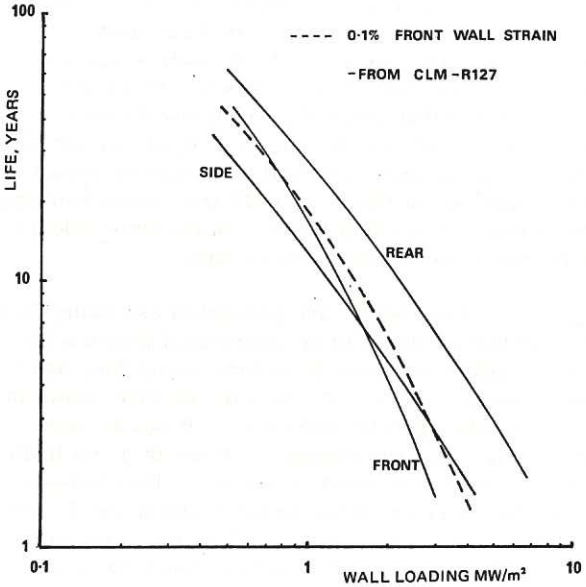

Fig.9 Comparison of 0.1% irradiation creep strain at front, side and rear wall positions.

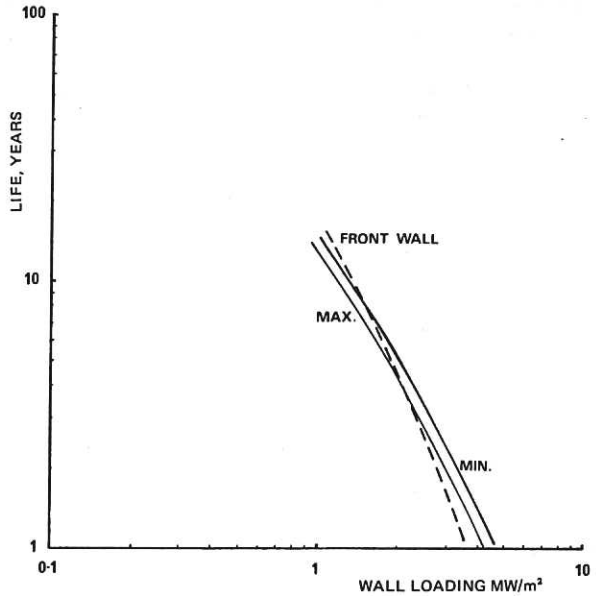

Fig.10 0.1% strain lines at the maximum and minimum damage points at an axial position 12cm from the front wall.

5. DISCUSSION

Figure 4 shows that for the side and rear wall positions the mid-wall temperature is virtually independent of wall loading while the front-wall temperature is a strong function of wall loading. Hence as the wall loading changes the estimate of strain for the front wall takes account of a considerable change in temperature but those for the side and rear walls do not. This accounts for the steeper slope of the 0.1% strain line for the front wall on Fig. 9. Figure 9 indicates that below a wall loading of about $1.6\,MW/m^2$, the greatest strain occurs in the side wall. For a 5 year life (at 100% load factor) the limiting wall loading is $1.8\,MW/m^2$.

Now the previous work presented the results of tests published on the change in material ductility with increasing fluence and related the exhaustion of ductility to irradiation creep strain in order to obtain a "design" line. These results indicated that the 0.1% strain line was a good approximation to the design line over the range of interest and it is proposed that that criterion is adopted here. It must be pointed out however, that the damage-rate in the front-wall is about a factor 2 higher than at the side wall, hence the available ductility there (ignoring any dependence on temperature) may be lower. If this factor is taken properly into account then it may be shown that conditions at the front-wall are always limiting. The authors do not feel there is sufficient evidence to be more conclusive on this point.

The results are presented assuming that the number of atoms in an interstitial loop n = 30. If the number of atoms in an interstitial loop had been chosen to be n = 10, then the picture shown in Fig. 9 would again be different. It can be seen from Fig. 5 that the change in strain in going from 350°C to 450°C is lower if n = 30. This follows from the variation of the factor f with n and T, see equation (1). With this assumption therefore the front-wall strain would have been limiting over the whole of the range of interest and the results as a whole would of course have been less pessimistic.

The limiting wall loading of $1.8\,MW/m^2$ is not greatly less than the figure $2.2\,MW/m^2$ obtained in the previous work (Ref. 1). The change may be accounted for by the temperature extrapolation of the creep data from 300°C to about 355°C indicated on Fig. 5.

6. CONCLUSIONS

(1) There is by no means unanimous agreement in the published literature on whether irradiation creep is a function of temperature or not.

(2) The relationship between irradiation creep and swelling suggested by Brailsford and Bullough is a possible means of extrapolating irradiation creep with temperature. A major uncertainty is the number of atoms in an interstitial loop nucleus.

(3) Extrapolations using Brailsford and Bullough for the reference cell show a reduction in the 5 year cell life wall loading from $2.2\,MW/m^2$ (Ref. 1) to $1.8\,MW/m^2$. The results emphasise the importance of maintaining the front wall temperature as low as possible.

(4) In the range of interest little difference in creep rate at the front and side walls is indicated. On the other hand there may be difference in ductility reduction at these positions which make the front-wall position limiting.

(5) Calculations are given which estimate the maximum circumferential variation of neutron damage-rate in the cell wall to have a value approaching 15% of the mean circumferential value and to occur at a depth of about 100 mm from the front wall of the most adversely positioned cell, with a corresponding resultant variation in irradiation creep. More refined calculations would tend to reduce rather than increase this estimate of circumferential variation.

(6) There are insufficient data on both irradiation creep and creep ductility to be able to determine an optimum temperature distribution in the cell. The calculations show that the temperature varies most with wall loading at the front of the cell and the general conclusion can be made that to minimise irradiation creep at the front wall, its temperature should be maintained as low as possible.

7. REFERENCES

1. STANBRIDGE, J.R. et al. Design of stainless steel blanket cells for a fusion reactor. CLM-R127. 1974.

2. GILBERT, E.R. In reactor creep of reactor materials. Reactor Technology Vol. 14 no. 3, 258 - 285. 1971.

3. HESKETH, R.V. Irradiation creep. BNES Conference on Irradiation Embrittlement and Creep. November 1972.

4. BRAILSFORD, A.D., BULLOUGH, R. Irradiation creep due to the growth of interstitial loops. Philosophical Magazine, Vol. 27 no. 1, 49 - 64. 1973.

5. MOSEDALE, D. et al. Further creep experiments in the Dounreay fast reactor. BNES Conference on Irradiation Embrittlement and Creep. November 1972.

6. LEWTHWAITE, G.W. Irradiation creep during void production. Journal of Nuclear Materials, Vol. 46,324 - 328. 1973.

7. OKAMOTO, P.R., HARKNESS, S.D. Stress biassed loop nucleation in irradiated Type 316 stainless steel. Journal of Nuclear Materials, Vol. 48, No. 2, 204-206. 1973.

8. HERSCHBACH, K., SCHNEIDER, W. Interconnection between irradiation creep and interstitial loop formation in fcc metals. Journal of Nuclear Materials, Vol. 51, No. 2, 215-220. 1974.

9. BRAGER, H.R., STRAALSUND, J.L. Defect development in neutron irradiated Type 316 stainless steel. Journal of Nuclear Materials, Vol. 46, 134-158. 1973.

10. WIFFEN, F.W., BLOOM, E.E. Effect of helium content on stainless steel swelling. ORNL-TM-4541. 1974.

11. BARNES, R.S. A theory of swelling and gas release for reactor materials. Journal of Nuclear Materials Vol 11, No2 135-148. 1964.

12. DANNER, W. Neutron flux asymmetry in toroidal geometries. Max Planck Institute for Plasma Physics. Report No. IPP 4/101. September 1972.

13. CONSTANTINE, G. Private communication February, 1975.

14. MITCHELL, J.T.D. Private communication 10th November, 1975.

15. KULCINSKI, G.L., DORAN, D.G., and ABDOU, M.A. Comparison of displacement and gas production rates in current fusion and future fusion reactors. UWFDM-15. April 1974.

APPENDIX A

A GRAPHICAL PROCEDURE FOR DETERMINING 14 MeV BLANKET FLUXES AT THE CELL SURFACES

The procedure utilises the scaled elevation of a portion of the blanket shown in Fig. 2, in which a batch of cylindrical cells is represented by close-packed circles. Points 'A' and 'B' in this Figure then represent the traces along the side-wall of a given cell of points of circumferential maximum and minimum damage-rate respectively. Thus, assuming the angular distribution for the incident 14 MeV neutron current defined in the main text, all 14 MeV neutrons which intercept the maximum or minimum trace at any distance l into the blanket, will arrive at the first wall uniformly distributed within a circle having point 'A' or 'B' as centre, and of radius $\frac{3}{4}l$, ($\alpha = \tan^{-1}\frac{3}{4}$ being the maximum angle of incidence as shown in Fig. 3).

The total maximum or minimum flux at various values of l was found by first considering the appropriate circle to be subdivided radially and azimuthally into small segmental elements of the form shown in Fig. 2, and then scaling off a value for the solid material fraction, f, of the path from the centre of each of these elements to point 'A' or 'B'. Since f is independent of l, this scaling could be effected directly from Fig. 2 without the need for an additional elevation. Calling S the first wall 14 MeV current-density, and r, δr, $\delta\theta$ respectively the radius, and radial and azimuthal extents of the element, the 14 MeV neutron current crossing it was then assumed replaced by a point source of strength $Sr\,\delta r\,\delta\theta$ located at its centre, and having neutron flight directions uniformly distributed within a cone of half-angle $\hat{\alpha} = \tan^{-1}\frac{3}{4}$. The length of flight-path from such a point source location to an associated maximum or minimum point is then $(r^2+l^2)^{\frac{1}{2}}$. Assuming the normal exponential form for attenuation due to scattering and absorption when traversing blanket material, this source would produce at the maximum or minimum point considered a 14 MeV flux contribution of magnitude:

$$\frac{Sr\delta r\delta\theta}{2\pi r(r^2+l^2)^{\frac{1}{2}}(1-\cos\hat{\alpha})} \cdot \exp\left[\frac{-f(r^2+l^2)^{\frac{1}{2}}}{l_s}\right]$$

where l_s is the effective mean free path of 14 MeV neutrons in smeared blanket material (see main text).

The total maximum or minimum flux at each depth l considered could then be obtained by manually summing this expression over all segments in all contributing annuli. The annular width, δr, employed was 1 cm for $0 < r < 5$ cm and 5 cm for greater r. The segment azimuthal spread, $\delta\theta$, was $\pi/8$ at all radii.

Corresponding results for a fully homogeneous blanket were obtained by the same procedure as for points 'A' or 'B', but putting f = 1 throughout.

APPENDIX B

METHOD OF INTERPOLATING DAMAGE DUE TO NON 14 MeV FLUX AT VARIOUS DEPTHS THROUGH BLANKET

The method employed rested on two initial assumptions as follows:

(a) The datum multi-group point-values of non-14 MeV flux, when weighted with their corresponding damage cross-sections could be summed into single-group values of non-14 MeV damage flux which could then be spatially interpolated using the standard 1-group neutron diffusion equation with a source-term derived from the datum values of 14 MeV flux.

(b) For the purpose of its use as source-term in this way, a 14 MeV flux distribution could with sufficient accuracy be derived by fitting the datum point-values of 14 MeV flux to the form

$$\frac{\phi_{pl}}{\phi_{p0}} = \exp(-kl)$$

where ϕ_{pl} signifies the 14 MeV flux at depth l from the front wall.

On the basis of these assumptions the following procedure was used to obtain the estimated variation with depth of non-14 MeV damage-rate in the front half of the blanket:

(1) Using the datum values of 14 MeV flux at 0 and 0.25 m a value of k as defined in assumption (b) was determined.

(2) A damage-weighted single-group form of non-14 MeV flux for the l = 0 and l = 0.25 m datum points was then calculated in accordance with assumption (a).

(3) Assuming the approximate boundary condition of zero non-14 MeV current at $l = \infty$, integration of the 1-group diffusion equation in slab-geometry with inclusion of a source-term of the exponential form given above, led to the following expression for the non-14 MeV damage-flux distribution:

$$\frac{\phi_{sl}}{\phi_{s0}} = A\exp(-\lambda l) + B\exp(-kl)$$

where ϕ_{sl} signifies the non-14 MeV damage flux at depth l.

In this equation, (k being already determined), A, B, and λ were evaluated by fitting the 2 datum values of damage flux calculated in (2) and by applying the assumption of zero non-14 MeV current at the first wall.

APPENDIX C

CALCULATION OF CONSTANT STRAIN LINES FOR A CYLINDRICAL FUSION REACTOR BLANKET CELL

Additional nomenclature not used in text:

- d cell diameter
- p_c cell internal pressure
- t cell wall thickness
- ϵ_{eq} equivalent creep strain in a biaxial stress system
- ϵ_θ circumferential creep strain

The calculation of irradiation creep strain is similar to the one described in Appendix 3 of Ref. 1 for a different irradiation creep equation.

The irradiation creep equation (equation (1) in main text) may be written as follows, putting the second term equal to unity:-

$$\epsilon_{eq} = f \times \left(\frac{\Delta V}{V}\right) \qquad (C1)$$

Now the expressions for equivalent strain (ϵ_{eq}) and equivalent stress (σ_{eq}) which must be substituted in f were derived in Appendix 3 of Ref. 1 for cylindrical geometry with an interstitial pressure as follows:-

$$\epsilon_\theta = \frac{\sqrt{3}}{2}\,\epsilon_{eq} \qquad \text{and} \qquad \sigma_{eq} = \frac{\sqrt{3}}{4}\,\frac{dp_c}{t} \qquad (C2)$$

The swelling is given by equation (2), substituting the damage function for fluence (equation (3)) to give the following relation

$$\frac{\Delta V}{V} = \frac{\pi}{6} \times 10^{-9} K(T) \left[(.9356 W D \tau)^{D(T)} \exp\{E(T)\} \right] \qquad (C3)$$

where K(T), D(T), and E(T) are functions of temperature which are defined in the main text.

Cell pressure is related to wall loading as discussed in Ref. 1 and the expression derived in that report is used here, i.e.

$$p_c = 0.032 W^{1.76} + 0.083 W + 0.2 \qquad (C4)$$

This is used in the expression (C2) which together with values of d = 30 cm and t = 0.45 cm gives

$$\sigma_{eq} = 0.924 W^{1.76} + 2.4 W + 5.77 \qquad (C5)$$

For constant values of σ and T, equation (C1) may be integrated, giving

$$\epsilon_{eq} = f \times \left(\frac{\Delta V}{V}\right) \qquad (C6)$$

Substituting for ϵ_{eq} from (C2) we have

$$\epsilon_\theta = \frac{\sqrt{3}}{2} \times f \times \left(\frac{\Delta V}{V}\right) \qquad (C7)$$

Now f may be determined for given values of W and T, using equation (C5), and putting $b = 2.5 \times 10^{-10}$m.

Boltzmann's constant $k = 1.380 \times 10^{-23} JK^{-1}$.

$\frac{\Delta V}{V}$ may be calculated from equation (C3) for a particular position within a cell.

The equation (C7) was programmed for the Hewlett Packard 65 hand held programmable calculating machine which enable a large number of results to be obtained. These were cross-plotted and then presented in the form of the constant strain lines of Figures 4, 5 and 6.

HER MAJESTY'S STATIONERY OFFICE

Government Bookshops

49 High Holborn, London WC1V 6HB
13a Castle Street, Edinburgh EH2 3AR
41 The Hayes, Cardiff CF1 1JW
Brazennose Street, Manchester M60 8AS
Wine Street, Bristol BS1 2BQ
258 Broad Street, Birmingham B1 2HE
80 Chichester Street, Belfast BT1 4JY

Government publications are also available through booksellers